Surfaces and Interfaces 72 (2025) 106928

Contents lists available at ScienceDirect

Surfaces and Interfaces

journal homepage: www.sciencedirect.com/journal/surfaces-and-interfaces

Deep level transient spectroscopy and theoretical modelling of defect states in few-layer MoS_2

Serhiy Kondratenko [a,*], Oleksandr I. Datsenko [a], Sergii Golovynskyi [b], Anastasiya Mykytiuk [a], Artem Kuklin [c], Hans Ågren [c], Volodymyr Dzhagan [a,d], Dietrich R.T. Zahn [e]

[a] Taras Shevchenko National University of Kyiv, 01601 Kyiv, Ukraine
[b] College of Physics and Optoelectronic Engineering, Shenzhen University, 518060 Shenzhen, PR China
[c] Department of Physics and Astronomy, Uppsala University, Box 516 SE-751 20, Uppsala, Sweden
[d] V. E. Lashkaryov Institute of Semiconductors Physics, NAS of Ukraine, 03028 Kyiv, Ukraine
[e] Semiconductor Physics and Research Center for Materials, Architectures and Integration of Nanomembranes (MAIN), Chemnitz University of Technology, D-09107 Chemnitz, Germany

ARTICLE INFO

Keywords:
Transition metal dichalcogenide, 2D material
MoS_2, Lattice defects, DLTS

ABSTRACT

Native defects can essentially affect the properties of semiconductors and devices based on them. The defect influence is critical for 2D materials obtained by mechanical exfoliation from layered crystals, as most defects may be introduced when exfoliating. A film of few-layer MoS_2 flakes on a SiO_2/Si substrate was studied using deep-level transient spectroscopy (DLTS). A set of electron traps with energy levels at 303, 440, and 633 meV below the conduction band was found. The values are compared to those obtained by the density functional theory calculations of most abundant point defects in bilayer MoS_2, such as Mo and S vacancies, Mo+*S* and S divacancies, or O substituting S in a surface S layer. Based on the calculation results, the three states found by DLTS were attributed to S vacancy (440 meV) and S divacancy (303 and 633 meV), being the most expected when preparing the layered 2D structures by mechanical exfoliation.

1. Introduction

Since the discovery of graphene, the whole universe of 2D materials has attracted immense attention. As the former has rather narrow or zero bandgap, hindering its use in nano-optoelectronics, other promising materials possessing a wider bandgap are of great interest. Due to the development of exfoliation techniques, there is a feasibility to obtain 2D materials from layered crystals, such as transition metal dichalcogenides (TMDCs), the intralayer binding energy of which is much higher than the interlayer one [1–3]. With indirect bandgap in bulk, they become direct-bandgap materials being thinned to monolayer (1L) sheets.

Molybdenum disulfide (MoS_2) is now one of the most studied 2D materials [4]. In the 1L case it has a fairly wide bandgap around 1.9 eV and can emit light in the visible range; thus, it is applicable as an active element in nano-optoelectronic devices [5–9]. Even though only 1L MoS_2 acquires a direct bandgap and is thus most intensively investigated [10,11], few-layer (FL) flakes exhibit satisfactory luminescent properties [12–15] and are also widely studied [16,17]. Moreover, the efficiency of thin 2D MoS_2 layers as light emitters and detectors can be enhanced in contact with metal [18–21] or semiconductor nanoparticles and quantum dots [22–27]. In addition, the photoelectric properties of 2D MoS_2 can be tuned by other ways of doping, e.g. excitation power [15,17,28,29] and energy [15,26,30], as well as heating [11,14,17,28] or mechanical strain. The effect of strain on doping and, hence, on the optical properties is well studied [30–35], since atomically-thin MoS_2 is considered as a promising material for flexible electronics.

It is known that 2D MoS_2 is intrinsically an *n*-type semiconductor due to inherent defects [36,37]. These defects also attract special attention, as they may essentially affect the properties and sometimes worsen the performance of MoS_2-based devices. The point defects and their complexes in 2D MoS_2 were observed by high-resolution electron microscopy [37–41], scanning tunneling microscopy [42–45], or X-ray photoelectron spectroscopy [46–49] and widely studied theoretically

* Corresponding author.
E-mail address: kondratenko@knu.ua (S. Kondratenko).

https://doi.org/10.1016/j.surfin.2025.106928
Received 21 October 2024; Received in revised form 20 May 2025; Accepted 11 June 2025
Available online 18 June 2025
2468-0230/© 2025 Elsevier B.V. All rights are reserved, including those for text and data mining, AI training, and similar technologies.

[38–40,50–52], when calculating such demanded parameters as formation energy and energy levels introduced into the band structure. Nevertheless, the experimental studies of the defect energy levels in 1L and FL MoS_2 by transient spectroscopies are rare [41] due to obvious difficulties in preparing the nanometer-thick samples with few-micrometer lateral sizes for the electrical measurements. Most of the recent deep level transition spectroscopy (DLTS) studies of MoS_2 were applied to bulk MoS_2 or at least multilayers of tens or hundreds of nanometer thickness [40,53].

In this work, we used DLTS to identify defect states in FL MoS_2 flakes, which were exfoliated from high-quality bulk crystals and deposited from the solution onto a SiO_2/Si substrate to form a thin film over few square millimeters. Electron traps with energy levels at 303, 440, and 633 meV below the conduction band edge (E_c) were found. Using the results of density functional theory (DFT) calculations, the traps were identified as S vacancy (V_S) and S divacancy (V_{S2}).

2. Methods

2.1. Sample preparation

To fabricate the Ag/MoS_2/SiO_2/*p*-Si structure for DLTS measurements, we used a commercially available (Graphene Laboratories Inc., USA) ethanol solution of MoS_2 flakes (18 mg/L) prepared using solution-based exfoliation. The range of flake thicknesses declared by the manufacturer was from 1 to 8 layers, and the lateral size varied from 100 to 400 nm (Fig. S1, Supplementary Materials). The positions of the A and B exciton peaks in the absorption spectra (Fig. S2) correspond to those characteristic for FL MoS_2 [54]. The flakes were deposited by spray-coating onto a *p*-Si (7.5 Ω·cm) substrate at 80 °C. The substrate was pre-cleaned by immersion into 48 % HF acid, forming a thin natural silicon oxide layer at the substrate surface during MoS_2 deposition in ambient air. The Raman spectrum of deposited MoS_2 shows the E^1_{2g} and A_{1g} Raman modes (Fig. S3), while the relatively wide frequency difference of ~24 cm^{-1} between them may evidence conglomeration of the flakes.

2.2. Deep level transition spectroscopy

To study the electrical properties of MoS_2/SiO_2/Si heterostructures, a 100-nm thick Ag circle electrode with area of ~7 mm^2 was deposited onto of the MoS_2 thin film in vacuum through a shadow mask with metal silver (99.99 % purity) pellets by thermal evaporation. The deposition pressure was $2.0 \cdot 10^{-5}$ Torr. The deposition rate (about 1 nm/s) was measured with a quartz crystal microbalance. An In/Ga eutectic back electrode was fabricated onto the back Si surface of the SiO_2/Si substrate at room temperature. The schematic of the obtained diode-like structure is displayed in Fig. 1a. An Ag/SiO_2/Si structure without MoS_2 was studied as a reference sample. The *C-V* and *J-V* characteristics of the device at different temperatures were investigated using an Agilent 4284A LCR meter and an Agilent 4156C Semiconductor Parameter Analyzer, respectively.

The energy spectrum of the defect states was studied using DLTS by a digital DLTS spectrometer FT-1030. Transient capacitance signals were detected with a 1 MHz capacitance meter (Boonton 72B C-meter). The DLTS spectra were obtained from Fourier transforms of the capacitance transients recorded as a function of temperature in the range of 80–320 K. This technique [55] is based on numerical Fourier transformation of the measured capacitance transients originated from the temperature-dependent kinetics of charge carrier release from in-gap states after filling them by electric pulses (Fig. 1b). The emission time constants were calculated from the maximum peaks of the Fourier coefficients versus temperature. After identifying all the peaks, an Arrhenius plot of ln ($\tau_{peak}T^2$) versus $1/kT$ yields the trap energies from the slope of the linear fit. The defect levels were filled by a 100 μs wide voltage pulse, $V_B = +0.5$ V, while the diode was under a reverse bias of $V_B = -1.0$ V before and after the pulse. The Schottky barrier at the interface near the top Ag contact, as well as the filling and release of the traps in the MoS_2 space charge area, are under positive and negative bias, respectively, as shown in Fig. 1b, where the band bending at the interfaces is schematically illustrated considering work functions of 5.2–5.4 eV for FL MoS_2 [56], 4.3 eV for Ag [57], 4.6–4.9 eV for Si [58], *p*-doping of the SiO_2/Si substrate and expected *n*-doping of FL MoS_2 and their bandgap widths of 1.1 and 1.4–1.6 eV [10], respectively.

3. Results and discussion

Capacitance-voltage (*C-V*) and current-voltage (*J-V*) characteristics were obtained at room temperature to evaluate the potential barrier in the formed Ag/MoS_2/SiO_2/Si heterostructure. The *C-V* and *J-V* plots of the Ag/MoS_2/SiO_2/Si and Ag/SiO_2/Si metal-insulator-semiconductor (MIS) diodes at 300 K are shown in Figs. 2a and 2b, respectively. The *J-V* curves are expectably nonlinear, i.e. the current under the forward bias (a negative potential to the MoS_2 film) was essentially higher than the current under the reverse bias. The rectifying behavior was observed for all studied temperatures indicating to the presence of the depletion layer in the silicon substrate. Furthermore, the reverse current of the MoS_2/SiO_2/Si MIS structure was one order less compared to that of the reference structure without the MoS_2 layer, obviously due to a higher potential barrier caused by a greater work function of MoS_2 compared to Si (a band schematic at Ag interface to SiO_2/Si is given in Figure S4 of Supplementary Materials).

We analyzed the *C-V* curve shapes measured using a probe signal frequency of 1 MHz to estimate the height of the potential barrier. The plots of $1/C^2$ versus voltage in Fig. 2a contain linear sections under the reverse bias (the deviations from the linearity are due to insufficient depletion at low voltages leading to a lower capacitance). Their intersections with the voltage axis indicate potential barrier heights of 109 and 373 meV for the Ag/SiO_2/Si and Ag/MoS_2/SiO_2/Si diodes, respectively. Consequently, the deposition of a MoS_2 film onto a *p*-type Si substrate causes a higher potential barrier than that in the reference diode.

DLTS spectra (the first order Fourier sine coefficient b_1 vs temperature) of the Ag/MoS_2/SiO_2/Si diode at different rate windows of 50 and

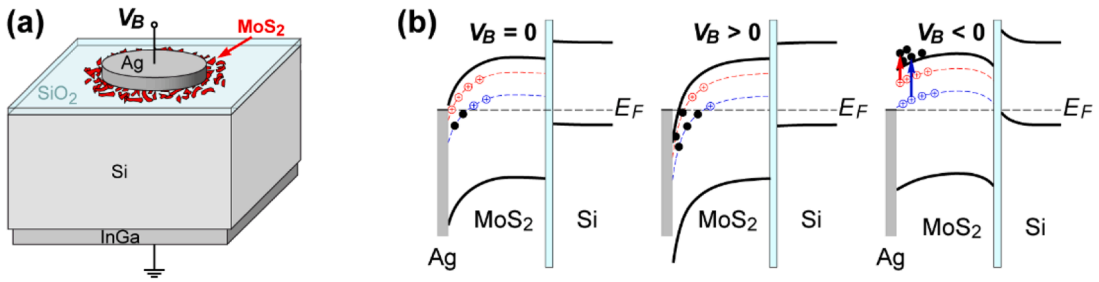

Fig. 1. (a) Diode-like structure with MoS_2 flakes for electrical and DLTS experiments; (b) band bending at MoS_2/Si interface with two types of traps at different biases (the carrier release contributing to the DLTS response is shown by arrows).

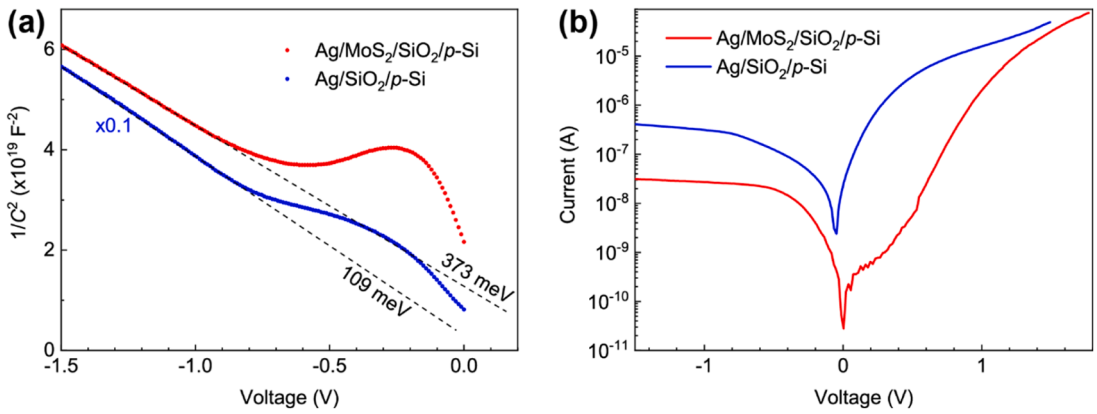

Fig. 2. *C-V* (a) and *J-V* (b) curves of the Ag/MoS_2/SiO_2/Si and Ag/SiO_2/Si MIS diodes at 300 K.

300 ms are shown in Fig. 3a. The dependences include three peaks, meaning that at least three trap states (energy levels) contribute to the spectra. Their positions are estimated from the slopes of the plots $\ln(\tau_{peak}T^2)$ versus $1/kT$ for different rate times, where τ_{peak} is the relaxation time at the temperature of the respective peak in the DLTS spectrum. Since the positive filling pulse ($U_F = +0.5$ V) fills the MoS_2 states by electrons, and the capacitance increases (positive transient signal), we may conclude that after injection electrons are released and traps are emptied. Therefore, the observed DLTS peaks are associated with electron traps. The plots for all three components shown in Fig. 3b are linear and give the positions of the electron levels in the MoS_2 film at $E_c - 303 \pm 5$, 440 ± 5, and 633 ± 5 meV. It is worth noting that the DLTS spectrum of the reference Ag/SiO_2/Si structure in Fig. 4a contains only one peak corresponding to a state positioned at $E_c - 377 \pm 5$ meV as follows from the Arrhenius plot in Fig. 4b. Studying the Ag/MoS_2/SiO_2/Si structure, this peak is obviously lost against the higher response of MoS_2 observed in Fig. 3a at the same temperatures.

As for identifying our electron traps, different kinds of V_S are the most probable origin. Indeed, they are most expected in MoS_2 flakes exfoliated from a high-quality bulk crystal, as each MoS_2 monolayer consists of an internal Mo layer and two external S layers, thus, the surface S layers are most possibly damaged when mechanically or chemically exfoliated. Furthermore, the formation energy of V_S is much lower than those of other point defects, except for S adatoms [39,50]. Estimations of the defect concentrations confirm these considerations. V_S are the most numerous defects not only in exfoliated flakes but also in CVD-grown ones [39]. This is a possible reason why MoS_2 reveals mainly electron conductivity without intentional doping [36,37].

To identify the defects that created the levels found in the experiment, DFT modeling of the energy band structure in a bilayer MoS_2 with different expectable defects was performed (Methods, Supplementary Materials). Apart from V_S and related complexes, the levels of V_{Mo} and of oxygen (O) substituting S (O_S) in an external layer were calculated. The calculated band structures are given in Fig. 5a and the respective densities of states (DOS) in Fig. 5b. The O_S defect is not found to introduce any states in the bandgap, while the levels introduced by V_{Mo} should be acceptors, thus, only V_S is of interest. It should be added that no contribution of Ag atoms to the DLTS response was considered, as Ag doping of MoS_2 was found to cause a *p*-doping of this material [59], while the DLTS signal polarity implies just donor-like responsible levels.

The states of the most expectable V_S in an external S layer are at E_c – 430/490 meV, while DOS shows a higher population of the deepest level. The location of V_S on an internal or external S layer affects the level position insignificantly, the states in an internal layer are estimated to be at 450/530 meV (its DOS is presented in Fig. 5b); however, such a defect is much less probable. A complex of two neighbor S vacancies (V_{S2} divacancy) in an S layer introduces two groups of states at E_c – 156/324 and ~600 meV; moreover, the DOS points out that these levels are populated. So, based on our calculations, we may attribute the found state E_c – 440 meV, which has the highest contribution to the DLTS signal, in FL MoS_2 to V_S in an external S layer. As for the two other states, at E_c – 303 and 633 meV, revealing lower responses in the DLTS spectra, we relate them to V_{S2}, which has an order lower content in 2D MoS_2, according to the estimations by Zhao et al. [41].

It is worth noting that other researchers also unquestionably related the experimentally found states at 270–360 meV to V_S [36,40,53], while Zhao et al. [41] attributed a state found at 632 meV also to V_S. Otherwise, we should note that, apart from the level at 270 meV related to V_S,

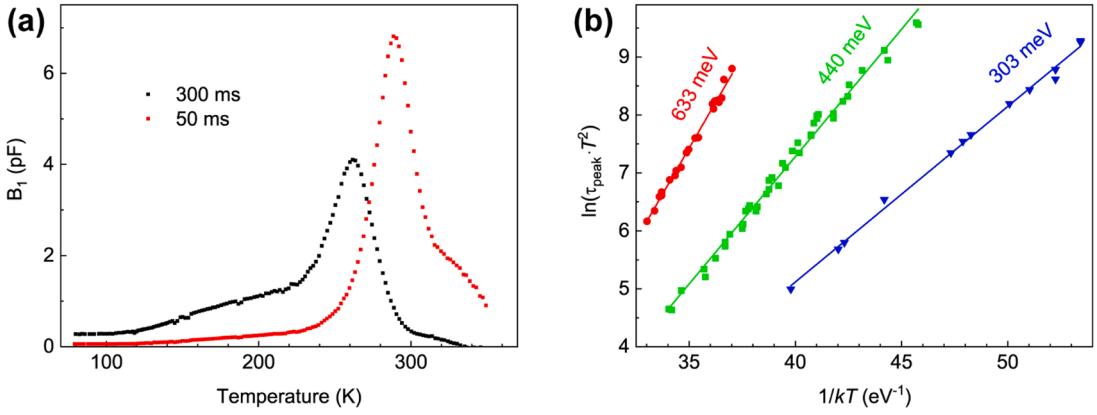

Fig. 3. (a) DLTS spectra of the Ag/MoS_2/SiO_2/Si diode obtained under filling pulse with an amplitude of $U_F = +0.5$ V and a width of 100 μs at different transient periods. (b) Arrhenius plot of the deep traps found in the spectra.

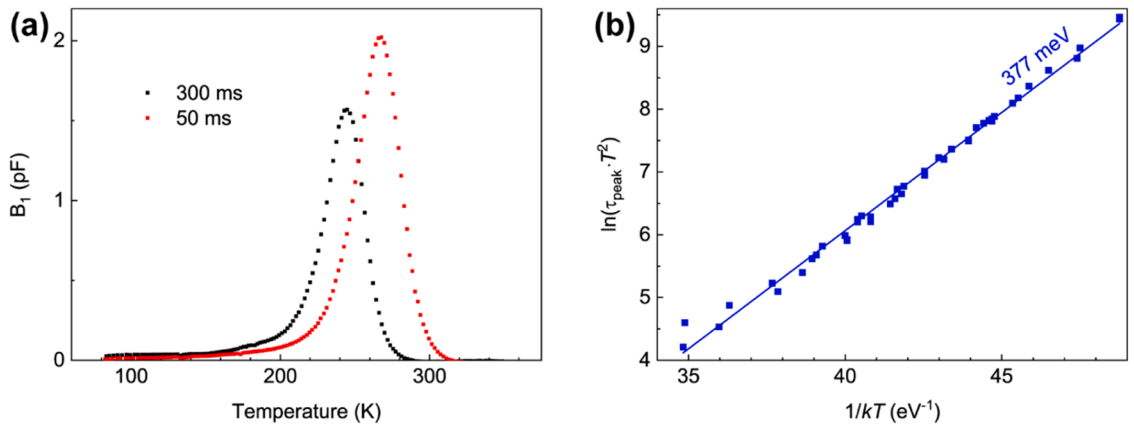

Fig. 4. (a) DLTS spectra of the reference Ag/SiO_2/Si diode obtained under filling pulse with an amplitude of $U_F = +0.5$ V and a width of 100 μs at different transient periods. (b) Arrhenius plot of the found state.

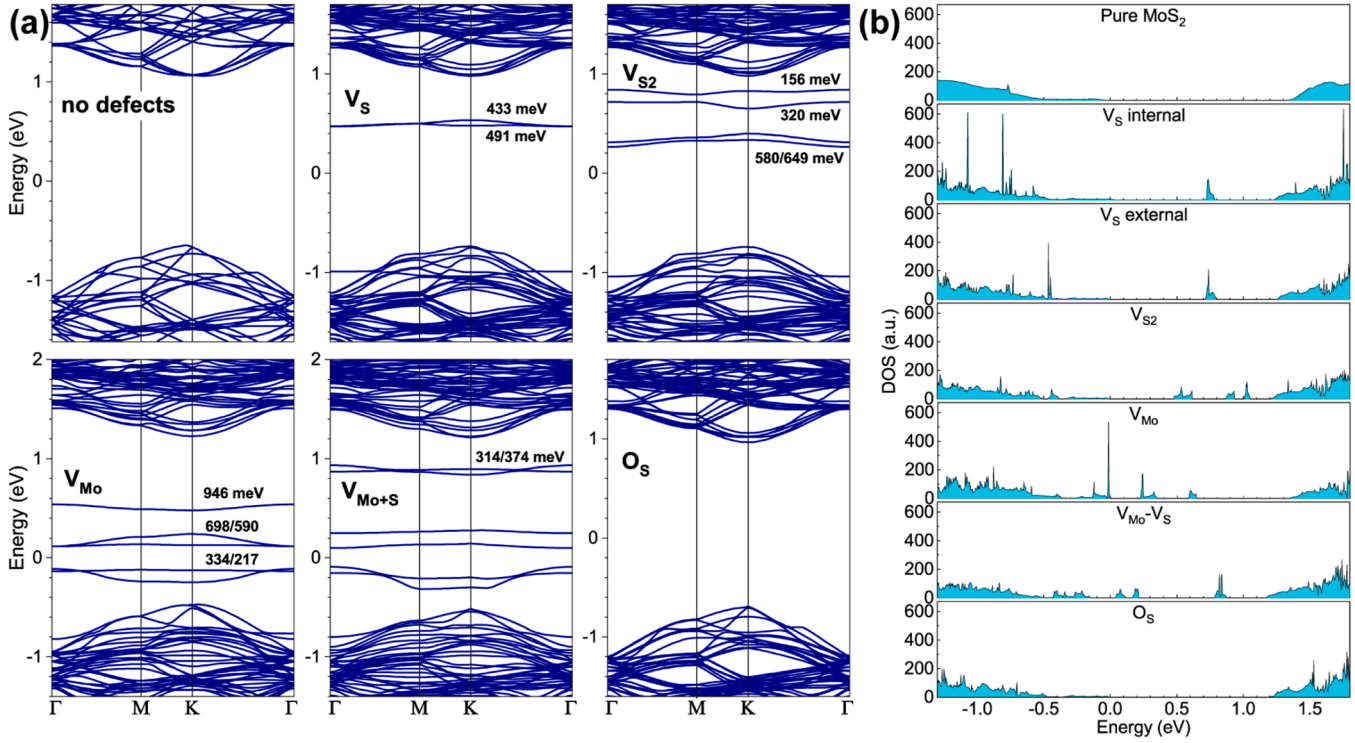

Fig. 5. DFT-calculated (a) band structure and (b) DOS of a perfect bilayer MoS_2 compared to that with different types of defects, the level depths below the conduction band near the K-point of the Brillouin zone are indicated nearby.

Ci et al. [40] detected a state at 440 meV and attributed it to a DX center, i.e. a complex consisting of a donor-like center and a vacancy. However, this state revealed that the DLTS response was several times less than that of V_S found there. Therefore, we cannot similarly identify our state with the same position at E_c – 440 meV.

So, the studied 2D-MoS_2 flakes demonstrate abundance of V_S, while no other defects are found with the DLTS technique. It should be emphasized that the detected DLTS signal from MoS_2 can be essentially lowered due to the natural oxidation of MoS_2 after exfoliation. Although MoS_2 crystal surface is stable to oxidation due to large energy barrier [60], V_S are easy passivated by oxygen, including atmospherical one [60,61]. As O_S defects introduce levels into the valence band rather than the bandgap [62] and induce *p*-conductivity in MoS_2 [63], the oxidation is considered as a promising way for elimination of the negative effect of V_S [62–65].

4. Conclusions

Defects in thin films of exfoliated FL MoS_2 flakes drop-casted onto a Si substrate were studied using the DLTS technique. Three electron traps with deep energy levels at E_c – 303, 440, and 633 eV were detected just in the film, while the pristine substrate revealed a different value of the activation energy. To identify the found level depths with native MoS_2 defects, DFT calculations of the most abundant point defects in bilayer MoS_2 were performed. Comparing to the calculated data, the energy states found by DLTS were attributed to S vacancy (440 eV) and S divacancy (303 and 633 eV), being most expected when preparing the layered 2D crystalline structures with S atoms at the external sides.

CRediT authorship contribution statement

Serhiy Kondratenko: Conceptualization, Resources, Methodology,

Investigation, Formal analysis, Writing – original draft, Supervision, Project administration, Funding acquisition. **Oleksandr I. Datsenko:** Formal analysis, Writing – original draft, Visualization. **Sergii Golovynskyi:** Formal analysis, Writing – original draft, Visualization. **Anastasiya Mykytiuk:** Investigation, Visualization, Writing – review & editing. **Artem Kuklin:** Formal analysis, Visualization, Writing – review & editing. **Hans Ågren:** Resources, Writing – review & editing. **Volodymyr Dzhagan:** Resources, Writing – review & editing. **Dietrich R.T. Zahn:** Resources, Writing – review & editing.

Declaration of competing interest

The authors declare that they have no known competing financial interests or personal relationships that could have appeared to influence the work reported in this paper.

Acknowledgments

The work is supported by the National Research Foundation of Ukraine (2023.03/0060).

Supplementary materials

Supplementary material associated with this article can be found, in the online version, at doi:10.1016/j.surfin.2025.106928.

Data availability

Data will be made available on request.

References

[1] R. Mas-Ballesté, C. Gómez-Navarro, J. Gómez-Herrero, F. Zamora, 2D materials: to graphene and beyond, Nanoscale 3 (1) (2011) 20–30.
[2] B. Guo, Q.l. Xiao, S.h. Wang, H. Zhang, 2D layered materials: synthesis, nonlinear optical properties, and device applications, Laser Photonics Rev 13 (12) (2019) 1800327.
[3] S. Golovynskyi, Nanomaterials for optoelectronics: an overview, Ukr. J. Phys. Opt. 25 (1) (2024) 01045–01053.
[4] F. Esposito, M. Bosi, G. Attolini, S. Golovynskyi, L. Seravalli, Two-dimensional MoS_2 for photonic applications, semiconductor physics, Quantum Electron. Optoelectron. 28 (01) (2025) 037–046.
[5] A.R. Klots, A.K.M. Newaz, B. Wang, D. Prasai, H. Krzyzanowska, J. Lin, D. Caudel, N.J. Ghimire, J. Yan, B.L. Ivanov, K.A. Velizhanin, A. Burger, D.G. Mandrus, N. H. Tolk, S.T. Pantelides, K.I. Bolotin, Probing excitonic states in suspended two-dimensional semiconductors by photocurrent spectroscopy, Sci. Rep. 4 (1) (2014) 6608.
[6] A. Sobhani, A. Lauchner, S. Najmaei, C. Ayala-Orozco, F. Wen, J. Lou, N.J. Halas, Enhancing the photocurrent and photoluminescence of single crystal monolayer MoS_2 with resonant plasmonic nanoshells, Appl. Phys. Lett. 104 (3) (2014) 031112.
[7] Z. Li, J. Chen, R. Dhall, S.B. Cronin, Highly efficient, high speed vertical photodiodes based on few-layer MoS_2, 2D Mater 4 (1) (2016) 015004.
[8] J. Shan, J. Li, X. Chu, M. Xu, F. Jin, X. Fang, Z. Wei, X. Wang, Enhanced photoresponse characteristics of transistors using CVD-grown MoS_2/WS_2 heterostructures, Appl. Surf. Sci. 443 (2018) 31–38.
[9] D. Vaquero, V. Clericò, J. Salvador-Sánchez, A. Martín-Ramos, E. Díaz, F. Domínguez-Adame, Y.M. Meziani, E. Diez, J. Quereda, Excitons, trions and Rydberg states in monolayer MoS_2 revealed by low-temperature photocurrent spectroscopy, Commun. Phys. 3 (1) (2020) 194.
[10] K.F. Mak, C. Lee, J. Hone, J. Shan, T.F. Heinz, Atomically thin MoS_2: a new direct-gap semiconductor, Phys. Rev. Lett. 105 (13) (2010) 136805.
[11] J.W. Christopher, B.B. Goldberg, A.K. Swan, Long tailed trions in monolayer MoS_2: temperature dependent asymmetry and resulting red-shift of trion photoluminescence spectra, Sci. Rep. 7 (1) (2017) 14062.
[12] R. Ganatra, Q. Zhang, Few-layer MoS_2: a promising layered semiconductor, ACS Nano 8 (5) (2014) 4074–4099.
[13] J.G. Kim, W.S. Yun, S. Jo, J. Lee, C.-H. Cho, Effect of interlayer interactions on exciton luminescence in atomic-layered MoS_2 crystals, Sci. Rep. 6 (1) (2016) 29813.
[14] S. Golovynskyi, I. Irfan, M. Bosi, L. Seravalli, O.I. Datsenko, I. Golovynska, B. Li, D. Lin, J. Qu, Exciton and trion in few-layer MoS_2: thickness- and temperature-dependent photoluminescence, Appl. Surf. Sci. 515 (2020) 146033.
[15] S. Golovynskyi, O.I. Datsenko, D. Dong, Y. Lin, I. Irfan, B. Li, D. Lin, J. Qu, Trion binding energy variation on photoluminescence excitation energy and power during direct to indirect bandgap crossover in monolayer and few-layer MoS_2, J. Phys. Chem. C. 125 (32) (2021) 17806–17819.
[16] J. Pei, J. Yang, R. Xu, Y.-H. Zeng, Y.W. Myint, S. Zhang, J.-C. Zheng, Q. Qin, X. Wang, W. Jiang, Y. Lu, Exciton and trion dynamics in bilayer MoS_2, Small 11 (48) (2015) 6384–6390.
[17] P.J. Ko, A. Abderrahmane, T.V. Thu, D. Ortega, T. Takamura, A. Sandhu, Laser power dependent optical properties of mono- and few-layer MoS_2, J. Nanosci. Nanotechno. 15 (9) (2015) 6843–6846.
[18] S. Catalán-Gómez, S. Garg, A. Redondo-Cubero, N. Gordillo, A. Andres, F. Nucciarelli, S. Kim, P. Kung, J. Pau, Photoluminescence enhancement of monolayer MoS_2 using plasmonic gallium nanoparticles, Nanoscale Adv 1 (2019) 884–893.
[19] Z. Luo, H. Jia, L. Lv, Q. Wang, X. Yan, Gate-tunable trion binding energy in monolayer MoS_2 with plasmonic superlattice, Nanoscale 12 (34) (2020) 17754–17761.
[20] I. Irfan, S. Golovynskyi, M. Bosi, L. Seravalli, O.A. Yeshchenko, B. Xue, D. Dong, Y. Lin, R. Qiu, B. Li, J. Qu, Enhancement of raman scattering and exciton/trion photoluminescence of monolayer and few-layer MoS_2 by Ag nanoprisms and nanoparticles: shape and size effects, J. Phys. Chem. C. 125 (7) (2021) 4119–4132.
[21] I. Irfan, S. Golovynskyi, O.A. Yeshchenko, M. Bosi, T. Zhou, B. Xue, B. Li, J. Qu, L. Seravalli, Plasmonic enhancement of exciton and trion photoluminescence in 2D MoS_2 decorated with Au nanorods: impact of nonspherical shape, Physica E. 140 (2022) 115213.
[22] D. Kufer, I. Nikitskiy, T. Lasanta, G. Navickaite, F.H.L. Koppens, G. Konstantatos, Hybrid 2D-0D MoS_2-PbS quantum dot photodetectors, Adv. Mater. 27 (1) (2015) 176–180.
[23] Z. Li, R. Ye, R. Feng, Y. Kang, X. Zhu, J.M. Tour, Z. Fang, Graphene quantum dots doping of MoS_2 monolayers, Adv. Mater. 27 (35) (2015) 5235–5240.
[24] D. Kufer, T. Lasanta, M. Bernechea, F.H.L. Koppens, G. Konstantatos, Interface engineering in hybrid quantum dot–2D phototransistors, ACS Photonics 3 (7) (2016) 1324–1330.
[25] L.P.L. Mawlong, A. Bora, P.K. Giri, Coupled charge transfer dynamics and photoluminescence quenching in monolayer MoS_2 decorated with WS_2 quantum dots, Sci. Rep. 9 (1) (2019) 19414.
[26] S. Golovynskyi, O.I. Datsenko, D. Dong, Y. Lin, I. Golovynska, Z. Jin, B. Li, H. Wu, MoS_2 monolayer quantum dots on a flake: efficient sensitization of exciton and trion photoluminescence via resonant nonradiative energy and charge transfers, Appl. Surf. Sci. 601 (2022) 154209.
[27] S. Kondratenko, O.I. Datsenko, D. Babich, V. Dzhagan, Y. Pan, M. Rahaman, O. Selyshchev, D.R.T. Zahn, Enhanced photoconductivity of hybrid 2D-QD MoS_2–$AgInS_2$ structures, J. Chem. Phys. 159 (4) (2023) 044707.
[28] T. Korn, S. Heydrich, M. Hirmer, J. Schmutzler, C. Schüller, Low-temperature photocarrier dynamics in monolayer MoS_2, Appl. Phys. Lett. 99 (10) (2011) 102109.
[29] D. Kaplan, Y. Gong, K. Mills, V. Swaminathan, P.M. Ajayan, S. Shirodkar, E. Kaxiras, Excitation intensity dependence of photoluminescence from monolayers of MoS_2 and WS_2/MoS_2 heterostructures, 2D Mater 3 (1) (2016) 015005.
[30] S. Golovynskyi, D. Dong, Y. Lin, O.I. Datsenko, B. Li, Hexagram bi-layer MoS_2 flake: the impact of polycrystallinity and strains on the exciton and trion photoluminescence, Surf. Interfaces 26 (2021) 101343.
[31] A. Castellanos-Gomez, R. Roldán, E. Cappelluti, M. Buscema, F. Guinea, H.S.J. van der Zant, G.A. Steele, Local strain engineering in atomically thin MoS_2, Nano. Lett 13 (11) (2013) 5361–5366.
[32] A. Michail, D. Anestopoulos, N. Delikoukos, J. Parthenios, S. Grammatikopoulos, S. A. Tsirkas, N.N. Lathiotakis, O. Frank, K. Filintoglou, K. Papagelis, Biaxial strain engineering of CVD and exfoliated single- and bi-layer MoS_2 crystals, 2D Mater 8 (1) (2020) 015023.
[33] O.I. Datsenko, S. Golovynskyi, A.I. Pérez-Jiménez, M. Chaigneau, A. Golovynskyi, I. Golovynska, V. Shevchenko, M. Bosi, L. Seravalli, Tensile strain creates trion: excitonic photoluminescence distribution over bilayer MoS_2 grown by CVD, Physica E. 154 (2023) 115812.
[34] L. Seravalli, F. Esposito, M. Bosi, L. Aversa, G. Trevisi, R. Verucchi, L. Lazzarini, F. Rossi, F. Fabbri, Built-in tensile strain dependence on the lateral size of monolayer MoS_2 synthesized by liquid precursor chemical vapor deposition, Nanoscale 15 (35) (2023) 14669–14678.
[35] S. Golovynskyi, O.I. Datsenko, A.I. Pérez-Jiménez, A. Kuklin, M. Chaigneau, A. Golovynskyi, I. Golovynska, M. Bosi, L. Seravalli, Exciton and trion at the perimeter and grain boundary of CVD-grown monolayer MoS_2: strain effects influencing application in nano-optoelectronics, ACS Appl. Nano Mater. 7 (13) (2024) 15570–15582.
[36] Ł. Gelczuk, J. Kopaczek, P. Scharoch, K. Komorowska, M. Blei, S. Tongay, R. Kudrawiec, Probing defects in MoS_2 Van der Waals crystal through deep-level transient spectroscopy, Phys. status solidi (RRL) 14 (12) (2020) 2000381.
[37] H. Qiu, T. Xu, Z. Wang, W. Ren, H. Nan, Z. Ni, Q. Chen, S. Yuan, F. Miao, F. Song, G. Long, Y. Shi, L. Sun, J. Wang, X. Wang, Hopping transport through defect-induced localized states in molybdenum disulphide, Nat. Commun. 4 (1) (2013) 2642.
[38] W. Zhou, X. Zou, S. Najmaei, Z. Liu, Y. Shi, J. Kong, J. Lou, P.M. Ajayan, B. I. Yakobson, J.-C. Idrobo, Intrinsic structural defects in monolayer molybdenum disulfide, Nano Lett 13 (6) (2013) 2615–2622.
[39] J. Hong, Z. Hu, M. Probert, K. Li, D. Lv, X. Yang, L. Gu, N. Mao, Q. Feng, L. Xie, J. Zhang, D. Wu, Z. Zhang, C. Jin, W. Ji, X. Zhang, J. Yuan, Z. Zhang, Exploring atomic defects in molybdenum disulphide monolayers, Nat. Commun. 6 (1) (2015) 6293.

[40] P. Ci, X. Tian, J. Kang, A. Salazar, K. Eriguchi, S. Warkander, K. Tang, J. Liu, Y. Chen, S. Tongay, W. Walukiewicz, J. Miao, O. Dubon, J. Wu, Chemical trends of deep levels in van der Waals semiconductors, Nat. Commun. 11 (1) (2020) 5373.
[41] Y. Zhao, M. Tripathi, K. Čerņevičs, A. Avsar, H.G. Ji, J.F. Gonzalez Marin, C.-Y. Cheon, Z. Wang, O.V. Yazyev, A. Kis, Electrical spectroscopy of defect states and their hybridization in monolayer MoS_2, Nat. Commun. 14 (1) (2023) 44.
[42] P. Vancsó, G.Z. Magda, J. Pető, J.-Y. Noh, Y.-S. Kim, C. Hwang, L.P. Biró, L. Tapasztó, The intrinsic defect structure of exfoliated MoS_2 single layers revealed by scanning tunneling microscopy, Sci. Rep. 6 (1) (2016) 29726.
[43] I. Delač Marion, D. Čapeta, B. Pielić, F. Faraguna, A. Gallardo, P. Pou, B. Biel, N. Vujičić, M. Kralj, Atomic-scale defects and electronic properties of a transferred synthesized MoS_2 monolayer, Nanotechnology 29 (30) (2018) 305703.
[44] D.J. Trainer, J. Nieminen, F. Bobba, B. Wang, X. Xi, A. Bansil, M. Iavarone, Visualization of defect induced in-gap states in monolayer MoS_2, npj 2D Mater, Appl 6 (1) (2022) 13.
[45] K. Nisi, J.C. Thomas, S. Levashov, E. Mitterreiter, T. Taniguchi, K. Watanabe, S. Aloni, T.R. Kuykendall, J. Eichhorn, A.W. Holleitner, A. Weber-Bargioni, C. Kastl, Scanning probe spectroscopy of sulfur vacancies and MoS_2 monolayers in side-contacted van der Waals heterostructures, 2D Mater. 12 (1) (2024) 015023.
[46] S. McDonnell, R. Addou, C. Buie, R.M. Wallace, C.L. Hinkle, Defect-dominated doping and contact resistance in MoS_2, ACS Nano. 8 (3) (2014) 2880–2888.
[47] A. Syari'ati, S. Kumar, A. Zahid, A.Ali El Yumin, J. Ye, P. Rudolf, Photoemission spectroscopy study of structural defects in molybdenum disulfide (MoS_2) grown by chemical vapor deposition (CVD), Chem. Commun. 55 (70) (2019) 10384–10387.
[48] D. Rana, S. Dahal, B. Sinkovic, Time evolution of the defect states at the surface of MoS_2, J. Appl. Phys. 135 (6) (2024) 064301.
[49] M. Rajput, S.K. Mallik, S. Chatterjee, A. Shukla, S. Hwang, S. Sahoo, G.V.P. Kumar, A. Rahman, Defect-engineered monolayer MoS_2 with enhanced memristive and synaptic functionality for neuromorphic computing, Commun. Mater. 5 (1) (2024) 190.
[50] S. Kc, R.C. Longo, R. Addou, R.M. Wallace, K. Cho, Impact of intrinsic atomic defects on the electronic structure of MoS_2 monolayers, Nanotechnology 25 (37) (2014) 375703.
[51] H.-P. Komsa, A.V. Krasheninnikov, Native defects in bulk and monolayer MoS_2 from first principles, Phys. Rev. B. 91 (12) (2015) 125304.
[52] N. Tsunetomo, S. Iguchi, M. Wierzbowska, A. Ueda, Y. Won, S. Heo, Y. Jeong, Y. Wakayama, K. Marumoto, Spin-states in MoS_2 thin-film transistors distinguished by operando electron spin resonance, Commun. Mater. 2 (1) (2021) 27.
[53] J.Y. Kim, Ł. Gelczuk, M.P. Polak, D. Hlushchenko, D. Morgan, R. Kudrawiec, I. Szlufarska, Experimental and theoretical studies of native deep-level defects in transition metal dichalcogenides, npj 2D mater, Appl 6 (1) (2022) 75.
[54] V. Bansal, V. Forsberg, R. Zhang, J. Bäckström, C. Dahlström, B. Andres, M. Norgren, M. Andersson, M. Hummelgård, H. Olin, Exfoliated MoS_2 in water without additives, Plos One 11 (4) (2016) e0154522.
[55] S. Weiss, R. Kassing, Deep level transient fourier spectroscopy (DLTFS) - A technique for the analysis of deep level properties, Solid-State Electron 31 (12) (1988) 1733–1742.
[56] S. Choi, Z. Shaolin, W. Yang, Layer-number-dependent work function of MoS_2 nanoflakes, J. Korean. Phys. Soc. 64 (10) (2014) 1550–1555.
[57] Y. Liu, J. Guo, E. Zhu, L. Liao, S.-J. Lee, M. Ding, I. Shakir, V. Gambin, Y. Huang, X. Duan, Approaching the Schottky–Mott limit in van der Waals metal–semiconductor junctions, Nature 557 (7707) (2018) 696–700.
[58] G. Shao, Work function and electron affinity of semiconductors: doping effect and complication due to Fermi level pinning, Energy Environ. Mater. 4 (3) (2021) 273–276.
[59] M. Kamruzzaman, J.A. Zapien, R. Afrose, T.K. Anam, M. Rahman, M.N.H. Liton, M. A. Helal, M.K.R. Khan, A.Ayotunde Emmanuel, A comparative study of Ag doping effects on the electronic, optical, carrier conversion, photocatalytic and electrical properties of MoS_2, Mater. Sci. Eng. B. 273 (2021) 115442.
[60] S. Kc, R.C. Longo, R.M. Wallace, K. Cho, Surface oxidation energetics and kinetics on MoS_2 monolayer, J. Appl. Phys. 117 (13) (2015) 135301.
[61] P. Afanasiev, C. Lorentz, Oxidation of nanodispersed MoS_2 in ambient air: the products and the mechanistic steps, J. Phys. Chem. C. 123 (12) (2019) 7486–7494.
[62] H. Yan, H. Chen, X. Cui, Q. Guan, B. Wang, Y. Cai, Unraveling energetics and states of adsorbing oxygen species with MoS_2 for modulated work function, Nanoscale Horizons 10 (2) (2025) 359–368.
[63] A.T. Neal, R. Pachter, S. Mou, P-type conduction in two-dimensional MoS_2 via oxygen incorporation, Appl. Phys. Lett. 110 (19) (2017) 193103.
[64] X. Zhang, J. Xu, A. Zhi, J. Wang, Y. Wang, W. Zhu, X. Han, X. Tian, X. Bai, B. Sun, Z. Wei, J. Zhang, K. Wang, Low-defect-density monolayer MoS_2 wafer by oxygen-assisted growth-repair strategy, Adv. Sci. 11 (42) (2024) 2408640.
[65] A. Wu, Q. Song, H. Liu, Oxygen atom adsorbed on the sulphur vacancy of monolayer MoS_2: a promising method for the passivation of the vacancy defect, Comput. Theor. Chem. 1187 (2020) 112906.